Available online at www.sciencedirect.com
SCIENCE DIRECT
Journal of Crystal Growth 287 (2006) 532–535
JOURNAL OF CRYSTAL GROWTH
www.elsevier.com/locate/jcrysgro

Optical and electrical characterization of OMVPE-grown AlGaAsSb epitaxial layers on InP substrates

T.S. Rao[a], M.G. So[a], W.Y. Jiang[a], T. Mayer[a], S. Roorda[b], S.C. Gujrathi[b], M.L.W. Thewalt[a], C.R. Bolognesi[c], S.P. Watkins[a,*]

[a] *Department of Physics, Simon Fraser University, 8888 University Drive, Burnaby, BC, Canada*
[b] *Département de Physique, Université de Montréal, Que., Canada*
[c] *Department of Physics and School of Engineering Science, Simon Fraser University, Burnaby, BC, Canada*

Abstract

Coherently strained $Al_xGa_{1-x}As_ySb_{1-y}$ epitaxial layers were grown over the range $0<x<0.2$ and $y\sim0.5$ on InP substrates by organometallic vapor phase epitaxy (OMVPE). The Al distribution coefficient was found to be much less than unity and this was attributed to reactions between trimethylaluminum and trimethylantimony at the growth temperature of 550 °C. Low-temperature photoluminescence (PL) spectra for $Al_xGa_{1-x}As_ySb_{1-y}$ showed single PL peaks for which the energy increased with increasing Al content in the layers in approximate agreement with theoretical predictions for the band gap of AlGaAsSb. P-type doping of AlGaAsSb up to $1.2\times10^{20}\,cm^{-3}$ was achieved using CBr_4. The growth rate of AlGaAsSb epilayers decreased with increasing CBr_4 dopant flow rates.
© 2005 Elsevier B.V. All rights reserved.

PACS: 81.05.Ea; 81.15.Gh; 78.20.−e

Keywords: A3. Metalorganic vapor phase epitaxy; B1. Antimonides; B2. Indium phosphide

1. Introduction

Antimony-based III–V compounds are attracting increased interest for optoelectronic applications as well as in high-speed devices. Much of the reported work in the organometallic vapor phase epitaxy (OMVPE) literature on the growth of AlGaAsSb was performed on GaSb substrates and has been aimed at photovoltaic applications and mid-IR lasers [1–4]. Growth of AlGaAsSb lattice matched to InP has been reported by molecular beam epitaxy (MBE) for high electron mobility transistors and for growth of Bragg reflector structures [5] and current confinement layers for lasers in the 1.55 μm region [6]. In a recent paper, we demonstrated the use of AlGaAsSb as an electron-blocking layer in GaAsSb/InP unitravelling carrier photodiodes grown on InP substrates by OMVPE [7].

In this paper, we report the OMVPE growth of $Al_xGa_{1-x}As_ySb_{1-y}$ epilayers on InP substrates under near-lattice-matched conditions ($y\sim0.50$), with varying Al compositions of x from 0 to 0.2. AlGaAsSb layers were characterized using low-temperature photoluminescence (PL) spectroscopy, X-ray diffractometry (XRD), and Hall effect measurements at 300 K. The effect of carbon doping using carbon tetrabromide (CBr_4) on the growth rate and the structural and electrical properties of AlGaAsSb was also studied.

2. Experiment

Epitaxial AlGaAsSb layers were grown in a vertical showerhead OMVPE reactor with a total H_2 flow of 5 SLM at a reactor pressure of 50 Torr. Trimethylindium (TMIn), trimethylaluminum (TMAl), tertiarybutylarsine (TBAs), tertiarybutylphosphine (TBP), trimethylantimony (TMSb) and triethylgallium (TEGa) were used as

*Corresponding author. Tel.: +1 604 291 5763; fax: +1 604 291 3592.
E-mail address: simonw@sfu.ca (S.P. Watkins).

0022-0248/$ - see front matter © 2005 Elsevier B.V. All rights reserved.
doi:10.1016/j.jcrysgro.2005.10.026

precursors. All epitaxial layers were grown at 550 °C. AlGaAsSb epilayers were grown on semi-insulating InP (0 0 1) exact oriented substrates. P-type doping of epilayers was performed using CBr_4. All epilayers were grown with a nominal V:III ratio of about 3.3. Aluminum mole fractions were determined by elastic recoil detection (ERD) in conjunction with time-of-flight [8]. High-energy heavy ions (30 MeV ^{35}Cl) were incident on the sample surface, 75° off-normal. Scattered ions and recoiled atoms exiting the sample surface were detected by a combined flight time and total energy detector oriented at 30° with respect to the ion beam. By measuring the flight time and total kinetic energy for each particle incident on the detector, the depth distribution of each element constituting the top-half micron of the sample surface can be determined without the need for an external standard. The energy loss parameters required for analyzing the data were obtained from TRIM 95 simulations [9]. As an internal check of self-consistency, the RBS signal of the scattered incident ions was compared with the energy distribution of recoiled atoms.

3. Results and discussion

Layers were grown at 550 °C, keeping the total group V molar ratio constant and the V/III ratio fixed at 3.31. Fig. 1 shows the relationship between vapor phase mole fraction x^{v}_{Al} and the solid phase mole fraction x in $Al_xGa_{1-x}As_ySb_{1-y}$. The Al distribution coefficient K_{Al} is defined as

$$K_{Al} = \{x/(1-x)\}/\{x^{v}_{Al}/(1-x^{v}_{Al})\}.$$

The solid composition x was measured using ERD. A least-squares fit to the data using the above expression yielded a distribution coefficient of $K = 0.18$. Such low distribution coefficients for Al have been previously reported for antimonide compounds. Wang [10] reported $K_{Al} < 1$ for AlGaAsSb grown on GaSb substrates which they attributed to the formation of an adduct between the Al and Sb sources. Koljonen et al. [11] reported $K_{Al} = 0.2$ for AlGaSb grown on GaSb substrates at 600 °C, and 0.8 for layers grown at 680 °C. They attributed this low value of the Al distribution coefficient to the lower deposition temperature resulting in partial decomposition of TMAl. In the present case, the AlGaAsSb epilayers were grown at 550 °C and it is possible that part of the observed low Al incorporation may also be due to the incomplete pyrolysis of TMAl at these low temperatures. Previous pyrolysis studies of TMAl for complete decomposition of TMAl ranged from 450 to 550 °C, depending on the ambient and surface [12,13].

Fig. 2 shows the relationship between the Al vapor phase mole fraction and the incorporation of Sb in the solid phase. The data were obtained from XRD fitting to a multilayer stack of 100 nm layers grown with identical As and Sb flows, but with different TMAl vapor phase mole fractions. The Sb solid phase mole fractions were obtained assuming pure GaAsSb. Because the mole fraction of Al was so low, the slight difference in lattice constant between AlGaAsSb and GaAsSb was neglected. A linear decrease in Sb solid composition is observed with increasing TMAl concentration, supporting the hypothesis of Wang et al. of interaction between the Al and Sb precursors [10]. This prereaction is the most likely origin of the low observed Al incorporation efficiency at 550 °C.

In Fig. 3 we have plotted the 4.2 K PL peak energies as a function of x in $Al_xGa_{1-x}As_ySb_{1-y}$ grown on InP substrates at near-lattice-matched conditions. The solid squares show data obtained using ERD for determination of x, while the open squares show data obtained using Auger profiling. The theoretical band gap values based on tabulated values of the band bowing parameters are also plotted in the same figure for $y = 0.5$. [14]. The ERD data show much better agreement with the expected band gap. We have not yet attempted to increase the Al content to higher values as the present device applications required

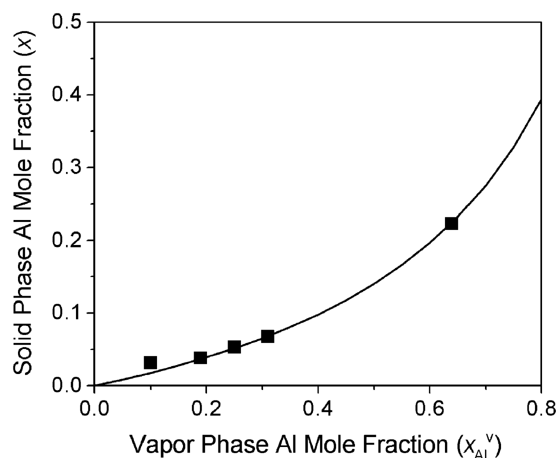

Fig. 1. Incorporation of Al in solid phase versus vapor phase for $Al_xGa_{1-x}As_{0.5}Sb_{0.5}$. Al compositions were measured by ERD.

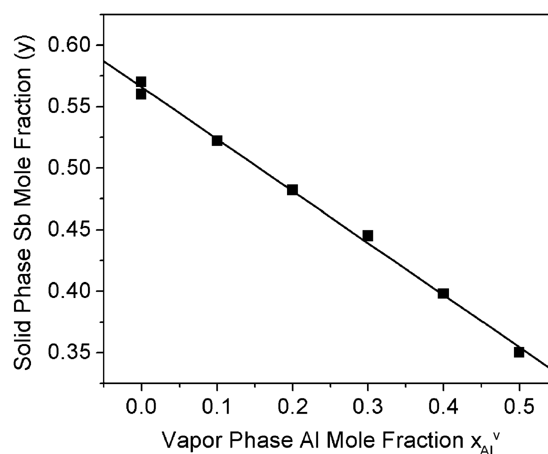

Fig. 2. Sb solid phase mole fraction y deduced from XRD measurements versus Al vapor phase mole fraction.

$x<0.2$. It is worth noting that other authors have seen fairly large discrepancies of up to 0.2 eV in the PL energies compared with predictions obtained using tabulated values of the bowing parameters [15]. We have also performed TEM measurements on these samples, which showed ordering in these quaternary material similar to the Cu–Au type observed in GaAsSb [16,17]. Recent PL measurements on GaAsSb ternary alloys indicated that the presence or absence of strong Cu–Au ordering had no effect on the PL energies [17].

We have studied the effect of p-type carbon doping on these layers using CBr_4 for potential application in graded layer HBT base layers. Fig. 4 shows the variation of growth rate of AlGaAsSb layers as a function of dopant flow rates for a solid phase Al composition of ~5%. The growth rate was observed to decrease from 0.23 to 0.16 nm/s as the CBr_4 flow rate increased from 0 to 70 sccm. The strong growth reduction in AlGaAsSb epilayers is matched with a reduction in the Sb incorporation. Similar results were also reported earlier for GaAsSb epilayers grown by OMVPE [18]. The observed etching effect of the halide dopant sources is attributed to the generation of halogen or hydrogen halide by thermal decomposition during the growth. Fig. 5 shows the variation of carrier concentration and Hall mobility with increasing dopant flow rates into the growth reactor for samples with an Al mole fraction of ~0.05. It can be seen from the figure that the p-type carrier concentration has increased from 1×10^{16} to $1.5\times10^{20}\,cm^{-3}$ as the CBr_4 flow rate increased from 0 to 60 sccm. A further increase of CBr_4 flow rates to 75 sccm has resulted in decrease of carrier concentration, indicating saturation behavior at this growth temperature. The Hall mobilities in these AlGaAsSb layers are comparable to those obtained in GaAsSb at comparable doping levels.

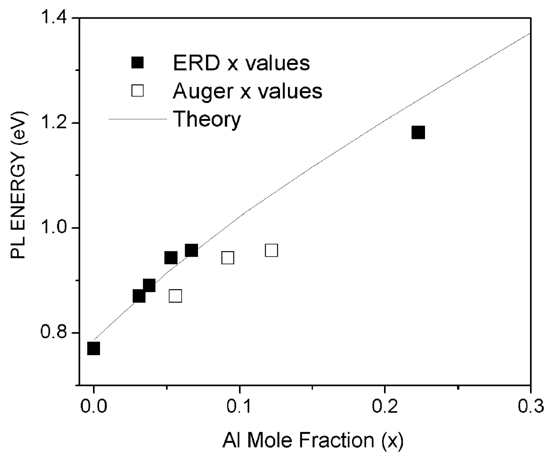

Fig. 3. PL energy for $Al_xGa_{1-x}As_{0.5}Sb_{0.5}$ versus Al solid phase composition x.

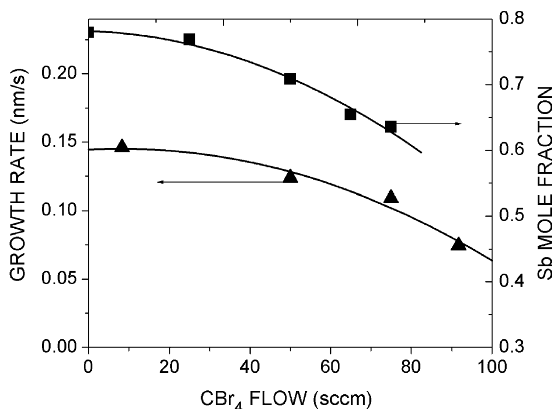

Fig. 4. Effect of carbon doping on the growth rate of AlGaAsSb. Al composition is ~0.05.

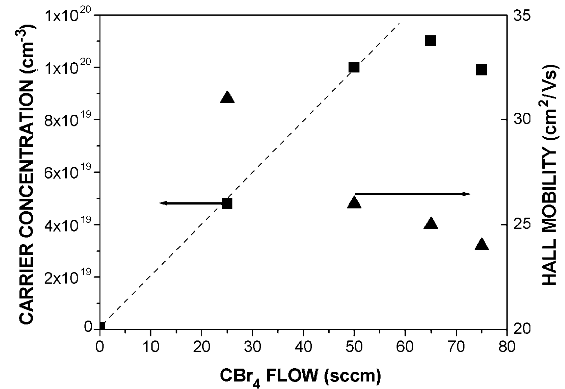

Fig. 5. Effect of carbon doping on the hole concentration in AlGaAsSb layers. Al composition is ~0.05.

4. Conclusions

AlGaAsSb epitaxial layers were grown on InP substrates using OMVPE. The Al distribution coefficient was found to be much less than unity and this was attributed to adduct formation between TMAl and TMSb. Low-temperature PL spectra for AlGaAsSb showed single PL peaks and the PL peak energy increased with increasing Al content in the layers from 0.76 for $x=0$ to 1.2 eV for $x=0.22$. The relationship between Al composition and PL energy roughly followed predictions obtained using accepted values of the band bowing parameters. P-type doping of AlGaAsSb was achieved using CBr_4. The growth rate of AlGaAsSb epilayers decreased with increasing CBr_4 dopant flow rates. A maximum p-type carrier concentration in the range of $1.2\times10^{20}\,cm^{-3}$ was achieved in the as-grown C-doped AlGaAsSb epilayers with mobility values close to those of GaAsSb.

Acknowledgments

Funding is acknowledged from the Natural Sciences and Engineering Research Council of Canada, le Fonds Québécois de la Recherche sur la Nature et les Technologies (Regroupement Québécois sur les Matériaux de Pointe), and Valorisation Recherche Québéc nanoQuébéc).

References

[1] C.A. Wang, J. Crystal Growth 272 (2004) 664.
[2] M.G. Mauk, V.M. Andreev, Semicond. Sci. Technol. 18 (2003) S191.
[3] J.G. Cederberg, et al., J. Crystal Growth 248 (2003) 289.
[4] H.K. Choi, S.J. Eglash, G.W. Turner, Appl. Phys. Lett. 64 (1994) 2474.
[5] G. Almuneau, et al., IEEE Photon. Technol. Lett. 12 (2000) 1322.
[6] M.H.M. Reddy, et al., J. Crystal Growth 251 (2003) 766.
[7] L. Zheng, et al., IEEE Photon. Technol. Lett. 17 (2005) 651.
[8] S.C. Gujrathi, ACS Symp. Ser. 440 (1990) 88.
[9] J.F. Ziegler, J.P. Biersack, U. Littmark, The Stopping and Ranges of Ions in Solids, First ed, Pergamon, New York, 1985, p. 321.
[10] C.A. Wang, J. Crystal Growth 170 (1997) 725.
[11] T. Koljonen, et al., J. Crystal Growth 169 (1996) 417.
[12] M. Mashita, Jpn. J. Phys. 29 (1990) 813.
[13] D.W. Squire, J. Vac. Sci. Technol. B 3 (1985) 1513.
[14] M. Linnik, Physica B 318 (2002) 140.
[15] S.P. Svensson, J. Appl. Phys. 81 (1997) 1422.
[16] H.R. Jen, M.J. Cherng, G.B. Stringfellow, Appl. Phys. Lett. 48 (1986) 1603.
[17] W.Y. Jiang, J.Q. Liu, M.G. So, T.S. Rao, M.L.W. Thewalt, K.L. Kavanagh, S.P. Watkins, Appl. Phys. Lett. 85 (2004) 5589.
[18] S.P. Watkins, O.J. Pitts, C. Dale, X.G. Xu, M.W. Dvorak, N. Matine, C.R. Bolognesi, J. Crystal Growth 221 (2000) 59.